Appendices

Contents

Appendices

A Effects on BTeV Sensitivities of Different Tevatron Bunch Spacings **A-1**
A.1 Introduction A-1
A.2 Effects on the Trigger A-3
A.2.1 The Detached Vertex Trigger A-3
A.2.2 The di-Muon Trigger A-4
A.3 Effects on the Charged Particle Tracking A-6
A.4 Effects on the Particle Identification by the Ring Imaging Cherenkov Counter (RICH) A-9
A.4.1 The Gas Radiator System A-9
A.4.2 The liquid radiator system A-13
A.5 Effects on the Reconstruction of π^o's and η's by the Electromagnetic Calorimeter A-14
A.5.1 Effects on $B \to \rho^+\pi^-$ due to changes in π^o's A-14
A.5.2 Effects on $B_s \to J/\psi\eta$ due to changes in η's A-15

Appendix A

Effects on BTeV Sensitivities of Different Tevatron Bunch Spacings

A.1 Introduction

The numbers of signal and background events have been evaluated for a year of BTeV running assuming a luminosity of $2 \times 10^{32}\text{cm}^{-2}\text{s}^{-1}$ and an effective duration of 10^7 seconds. This duration is about a factor of π smaller than the available time and colloquially is called a "Snowmass" year. This allows for two real effects. (1) The accelerator and detector will not run for a full year, as there must be time for repairs and maintenance. (2) The luminosity generally decays at a lifetime specific to each machine. The length of runs (or stores) is adjusted to maximize the total event yield taking into account the time necessary to establish new stores. Most of our studies were done taking the Tevatron to have 132 ns between beam bunches. It is likely that we will run with the current scheme of 396 ns between bunches.

A typical curve showing the current Tevatron luminosity is shown in Fig. A.1 [1]. This curve can be fit with a single exponential with a luminosity lifetime of about 13.5 hours. Stores last for about 20 hours. The average luminosity over a run is about 50% of the peak. The average number of interactions per crossing, $N_{Avg}(t)$, is proportional to the luminosity and at 396 ns bunch spacing, it can be parameterized as

$$N_{Avg}(T) = 6/T \times \int_{t=0}^{t=T} e^{-t/\tau} dt \quad , \tag{A.1}$$

where the lifetime τ is 13.5 hours. While this may change in the future, we base our study on this profile. Possible changes in the profile will not dramatically effect our conclusions.

At a luminosity of $2 \times 10^{32}\text{cm}^{-2}\text{s}^{-1}$ and the number of bunches of beam corresponding to a 396 ns separation of the bunches, there are an average of 6 interactions per crossing of the two beams. At 132 ns the average is 2 total interactions per crossing [2]. In both cases these numbers are means of Poisson distributions. In evaluating BTeV sensitivities it has been our practice to generate Monte Carlo events with these Poisson distributions without

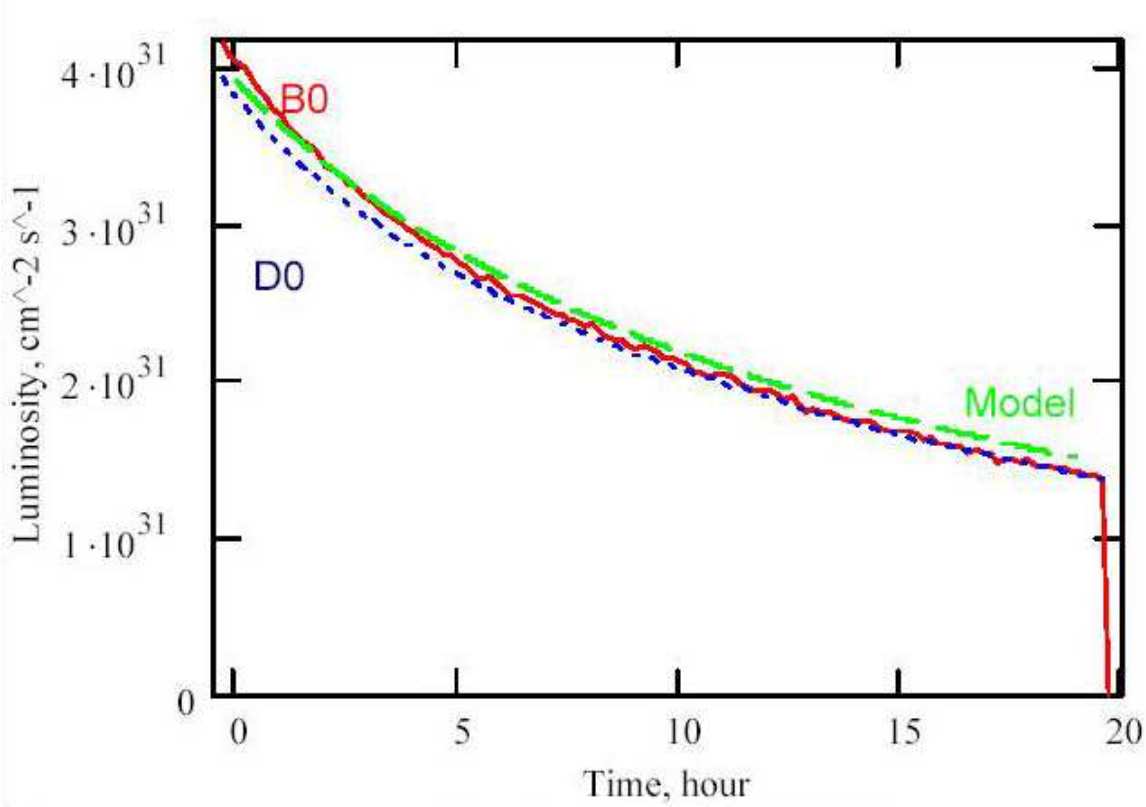

Figure A.1: The luminosity as a function of time for a typical Tevatron store for collisions at D0 and B0. Also shown is the result of a model prediction.

including the effects of the decrease of the luminosity with time. Most of our calculations were done at 132 ns. In this note we summarize the changes of going to 396 ns but here will include the effects of the luminosity decrease with time [3].

One way to approximate the effect of running at 396 ns on BTeV's physics sensitivities is to average the event efficiencies as a function of the number of interactions per crossing. Equation A.1 gives the mean number of interactions as a function of time. For the Tevatron we will start at ∼6 and end running at ∼2. This is closely approximated by a simple algorithm that the running at 396 ns will be 1/3 at 6 interactions per crossing, 1/3 at 4 and 1/3 at 2. Efficiencies have been simulated using BTeV GEANT. Running longer with a fill would give a lower average number of interactions per crossing, but might result in less total integrated luminosity. The actual running times will be optimized when the experiment begins taking data.

A.2 Effects on the Trigger

A.2.1 The Detached Vertex Trigger

The purpose of the BTeV Trigger System is to select data likely to include reconstructible beauty or charm decays. The goal is to record data for those beam crossings that contain events that would plausibly survive all the requirements of the BTeV data analysis programs and contribute to physics signals (as well as special calibration and monitoring data), while rejecting all other beam crossings. The trigger works by selecting interactions with tracks that do not point to the main interaction vertex. These tracks are required to have a minimum transverse momentum of 250 MeV to avoid candidates with large multiple scattering. Triggers are then made by taking n tracks each with cuts on the significance of detachment (in units of L/σ).

The results that we present, for a range of 2-6 interactions per beam crossing, come from studies of the different hardware components used in the Level 1 pixel trigger, efficiency for minimum bias and B_s interactions, and bandwidth studies for data flowing into Level 1 and bandwidth into Level 2 for interactions that satisfy the Level 1 pixel trigger requirements.

To perform the large number of calculations needed to process and select B events we require a massively parallel system with several thousand computational elements. These elements include large Field Programmable Gate Arrays (FPGAs), Digital Signal Processors (DSPs), and general-purpose microprocessors. FPGAs are used at the earliest stage of the processing pipeline to perform the large numbers of rudimentary calculations that are required for pattern recognition. DSPs offer more programming flexibility than FPGAs, and are used in the Level 1 trigger for the later stages of track reconstruction, and for vertex reconstruction.

Our studies of the FPGAs show that the time required to process pixel data increases almost linearly with the number of interactions per beam crossing. Although the timing for this part of the Level 1 hardware is not an important factor (since processing times are significantly higher for the DSPs), our studies do confirm that the algorithm behaves in a robust manner as the number of interactions per beam crossing increases. Our studies indicate that the requirements for memory resources for the FPGAs also increase linearly. This is not surprising, since each additional event in a beam crossing adds an equal amount of data. This is compensated by the fact that there is more time between beam crossings.

In Table A.1 we show the results of simulating the Level 1 pixel trigger for averages of 2, 4, and 6 interactions per beam crossing. Our nominal bandwidth into the second trigger level to 12.5 GB/s. At an average of two or six interactions per crossing this allows 2% of minimum bias crossing to pass the trigger. We quote results for the mode $B_s \to D_s^{\pm} K^{\pm}$ and expect other modes to show similar effects.

We choose the L/σ requirement for $n = 2$ detached tracks to trigger on only 2% of the minimum bias (non-B) crossings. Note that the L/σ cut, as well as other cuts, can be dynamically changed during the run. The trigger efficiency on this final state then goes from 79% to 75% to 66% as we go from 2 to 4 to 6 interactions per crossing. The average loss of

<Int/crossing>	L/σ	Bunch Spacing (ns)	$\epsilon(B_s \to D_s K)$	ϵ(Minimum bias)	Level 2 (GB/s)
2	1.9	132	0.79	0.020	12.5
4	3.2	396	0.75	0.020	8.4
4	2.3	396	0.78	0.035	14.6
6	4.7	396	0.66	0.020	12.5
6	3.6	396	0.71	0.030	18.8

Table A.1: Effects on trigger efficiencies from different average number of interactions per crossing. The last column refers to the data rate out of the Level 1 trigger into Level 2.

efficiency, therefore, taking 1/3 of the luminosity at 2, 4 and 6 interactions per crossing is 5.7% in absolute efficiency, i.e. a 7% effect on the signal size. The trigger system is specified with a requirement for a 50% overcapacity, including in the L2 input data rate. If we change the requirement on the L1 selection to meet the L2 data bandwidth instead of a straight 2% rejection of minimum bias crossings, we can improve the L1 trigger efficiency and reduce the effect of running at 396 ns to have only a signal reduction of 4% instead of 7%.

A.2.2 The di-Muon Trigger

We also trigger on events with two muon candidates in the final state. The main use of this trigger is to check the efficiency of the main detached vertex trigger. It is also useful for enhancing the number of $B \to X\mu^+\mu^-$ and $B \to J/\psi X$; $\psi \to \mu^+\mu^-$ events.

We have simulated the efficiency and rejection of the di-muon trigger scheme for $< N >$ = 2, 3, 4, and 5 interactions/crossing. (See the di-Muon trigger section in Part 4 of the TDR, 'Data Acquisition, Monitoring Contrl and Trigger Electronics' for more details.) The results are summarized in Fig. A.2.

We see that although efficiency is largely unaffected by increasing $< N >$, the minimum-bias rejection factor falls significantly. It is still true, however, that even for $< N >= 5$ we can achieve a rejection factor of 400 with 60% efficiency. This is well within BTeV's requirements on the efficiency and rejection of the muon trigger and will enable it to achieve its intended goals.

It is worth noting that significantly higher rejection as well as a much lower susceptibility to "non-muon" background hits can be achieved at the expense of efficiency by taking into account the very tight correlation between hit tubes in different views within a single station. This technique of "spacepoint" finding within some or all stations prior to correlating these hits between stations (the latter step being the approach described in detail above), was in fact the first algorithm studied in depth when developing the baseline design. While we are not using the spacepoint method in the current baseline design because of its inherently lower efficiency and slower execution speed, this can be revisited if we are faced background rates that are much worse than anticipated.

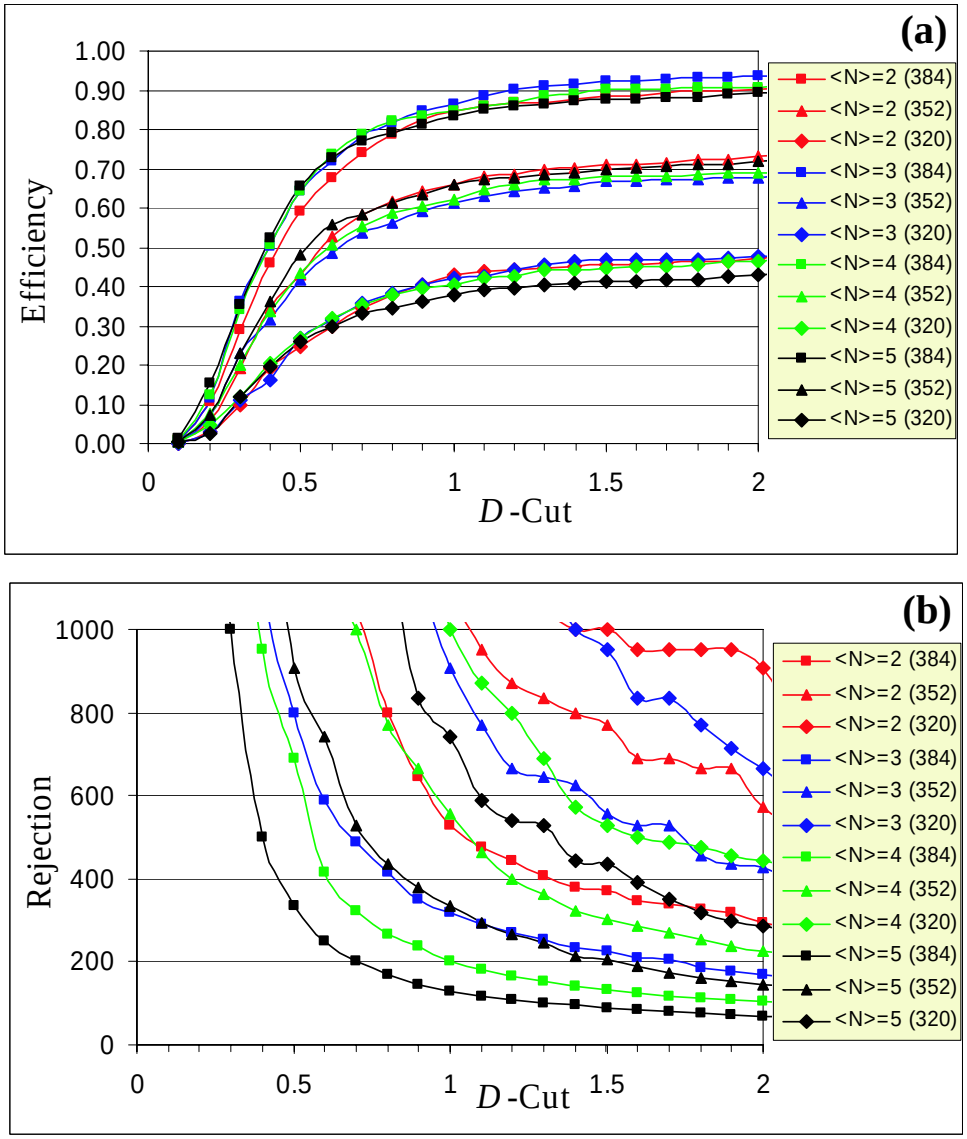

Figure A.2: (a) Efficiency for $J/\psi \to \mu^+\mu^-$ events and (b) rejection for minimum bias beam crossings using the "3/4" trigger scheme as a function of D-cut, where $D = d/\sigma$, and d is the distance of a hit to a good muon track plane defined by all the hits in a view σ is the standard deviation of the d distribution in that view. Shown are the results for various average minimum bias interactions per crossing $< N >$, as well as maximum tube number requirement. The large scatter of the points at high rejection values simply reflects low statistics.

A.3 Effects on the Charged Particle Tracking

Both the pixel detector and the silicon strip detector have such fine segmentation and the typical occupancies so small that there are no discernible effects on the tracking in these devices from the increased particle density due to more interactions per crossing. The pixel occupancy in the most active region is on the order of $\sim 10^{-4}$, while the silicon gets no worse than $\sim$2.4%, both at 2 interactions per crossing. The straw detector, however, has rather large elements 4 mm in diameter and several meter lengths allowing having high enough occupancies that possibly could be detrimental to the tracking.

The baseline forward silicon design has planes 27 cm x 27 cm. Enlarging the planes would lower occupancies and possibly increase tracking efficiencies in the straw detector without increasing significantly the silicon occupancies, since these are largest closest to the beam. We use an alternative design having silicon planes 40 cm $\times$ 40 cm, which is a convenient size for larger silicon, if desired.

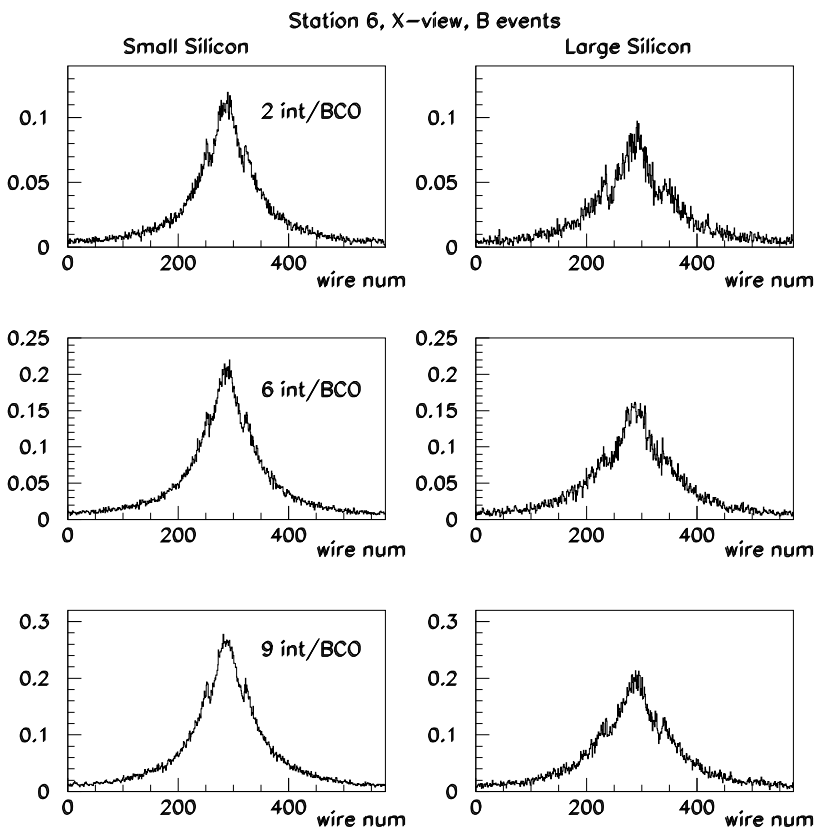

Figure A.3: Occupancy of Straw Station 6, X-view (non-bend plane) for a B interaction plus 2,6 or 9 minimum bias interactions. Left side: Dead area 27 cm $\times$ 27 cm; Right side: dead area 40 cm $\times$ 40 cm

Table A.2: Tracking efficiency for pixel seeded tracks (%)

	2 int/BCO		6 int/BCO		9 int/BCO	
	small FSil	big FSil	small FSil	big FSil	small FSil	big FSil
All tracks	97.6 ± 0.2	96.3 ± 0.2	96.1 ± 0.2	95.4 ± 0.2	95.1 ± 0.2	94.6 ± 0.2
B decay tracks	99.2 ± 0.5	97.7 ± 0.5	98.2 ± 0.5	97.5 ± 0.5	98.4 ± 0.5	96.8 ± 0.5

The combination of inner silicon and outer straw tracking is done at 7 "stations," 3 inside the magnet and 3 outside the magnet up to the RICH detector and one downstream of the RICH in front of the Electromagnetic Calorimeter. Station 6 is just before the RICH detector and here the straws subtend the largest fraction of the solid angle acceptance. Thus we chose to concentrate our studies on this station. Figure A.3 shows the occupancy of the Straw detector at Station 6 in the non-bend view (X) as a function of the distance to the beam line for a B interaction accompanied by a Poisson distributed average of 2 interactions per crossing and 6 interactions per crossing, corresponding to 132 ns and 396 ns bunch spacing respectively. We also include the case of 9 interactions per crossing, to view the consequences of even higher luminosity. While the occupancy is indeed smaller for the 40 cm $\times$ 40 cm silicon planes compared with the 27 cm $\times$ 27 cm planes, the occupancy in the center of the detector drops fractionally only by about 25% using the larger silicon planes.

To ascertain the effects of the increased occupancy we studied our ability to reconstruct charged tracks. We start with tracks that have hits in at least 4 pixel stations so that a seed track can be found in the pixel region and projected downstream to the forward tracking stations. Pixel seeded tracks are reconstructed by assuming perfect pattern recognition in the pixels, doing a Kalman fit and then projecting the track to the first forward tracking station. The closest hit to the projected track in each plane is added to the track if it is within a window of $\pm 4\sigma$ in the X-view or $\pm 6\sigma$ in the U and V-views. If all three planes of a straw view are hit then an attempt is made to resolve the left-right ambiguity, otherwise the wire position is used with a large error. The track is then projected to the next station and the process is iterated until the track reaches Station 7 or is outside the geometric acceptance of the Straw detector.

A track is considered to be reconstructed if its true momentum is above 3 GeV/c, the minimum needed to exit the spectrometer magnet, it has hits in at least 4 pixel stations and 4 downstream stations and its reconstructed momentum is within 3% of the true momentum. The efficiency is determined by comparing the number of tracks satisfying these requirements and found using the method described above with the number of tracks satisfying the same requirements using perfect pattern recognition. The results are shown in Table A.2. The efficiency is adequate even for 9 interactions/crossing and there is no improvement with larger silicon planes.

Next we consider the possible effects on momenta and mass resolutions. Fig. A.4 shows the momentum resolution distribution ($\Delta(p)/p$) for the case of 6 interactions per crossing.

Comparing the upper plot, which uses only the correct hits, and the lower plot where we actually reconstruct the track, we see no effect of the higher number of interactions.

Even the mass resolution for the all charged reaction, $B_s \to D_s^+ K^-$; $D_s^+ \to \phi\pi^+$, shown in Fig. A.5, shows little if any adverse affects.

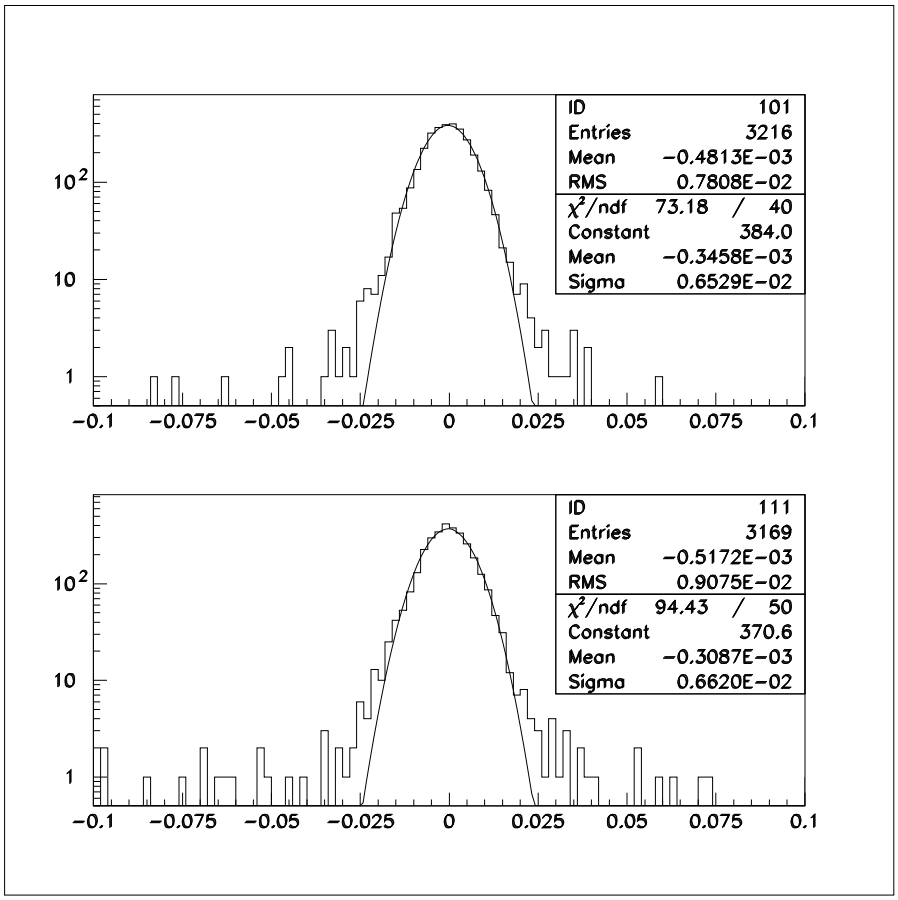

Figure A.4: Momentum resolution (Δ(p)/p), 6 interactions/crossing, silicon planes 27x27 cm, top: perfect tracking, bottom: track finding as described in text

We conclude that there is little effect on tracks through the pixels and straws due to the increased number of interactions per crossing and larger silicon is not needed.

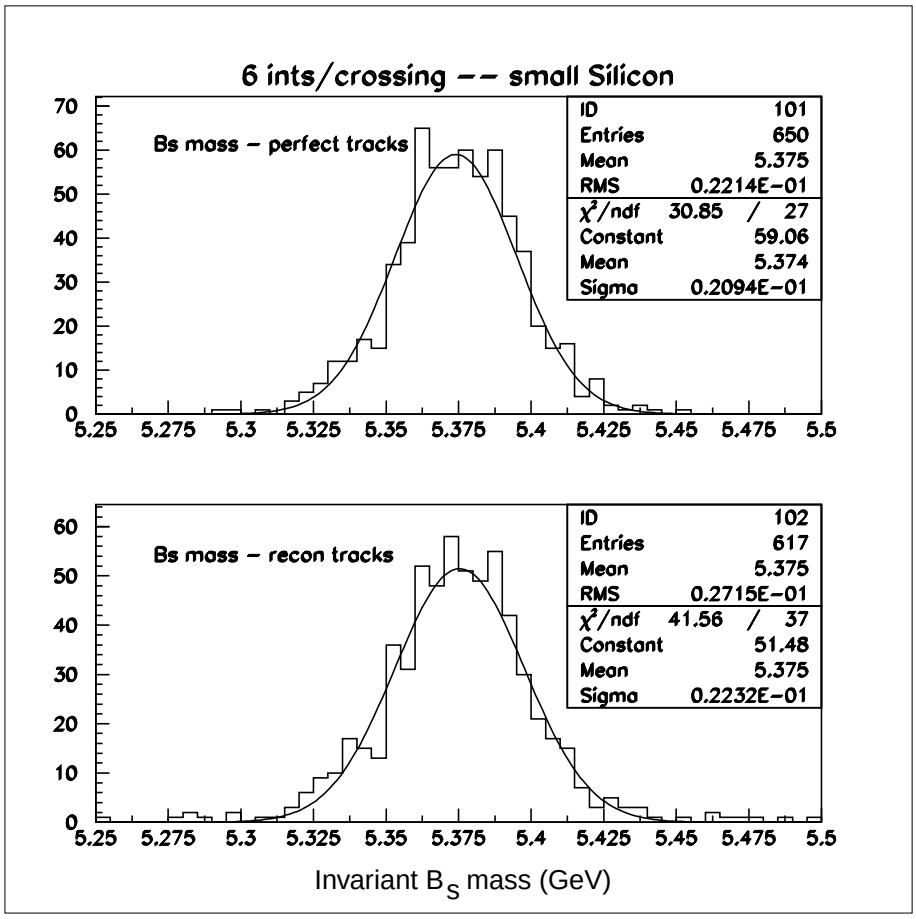

Figure A.5: B_s mass spectrum, 6 interactions/crossing, silicon planes 27 cm x 27 cm, top: perfect tracking, bottom: track finding as described in text.

A.4 Effects on the Particle Identification by the Ring Imaging Cherenkov Counter (RICH)

A.4.1 The Gas Radiator System

We look at the decay $B_S \to D_s^{\pm} K^{\mp}$, $D_s \to \phi\pi$, $\phi \to K^+K^-$ as a benchmark physics state needing good performance from the RICH for $K - \pi$ separation to measure the CKM angle γ. This decay has three charged kaons and one charged pion in the final state. We have done two separate and independent studies of this final state. In the first study, we require positive identification of the Kaon produced directly from the B_s and at least one of the two Kaons from the ϕ decay. The analysis is identical to that in the BTeV Proposal Update [4].

To see the effects of different numbers interactions per bunch, we did different simulations corresponding explicitly to different numbers of minimum bias events per bunch, *imin*, in

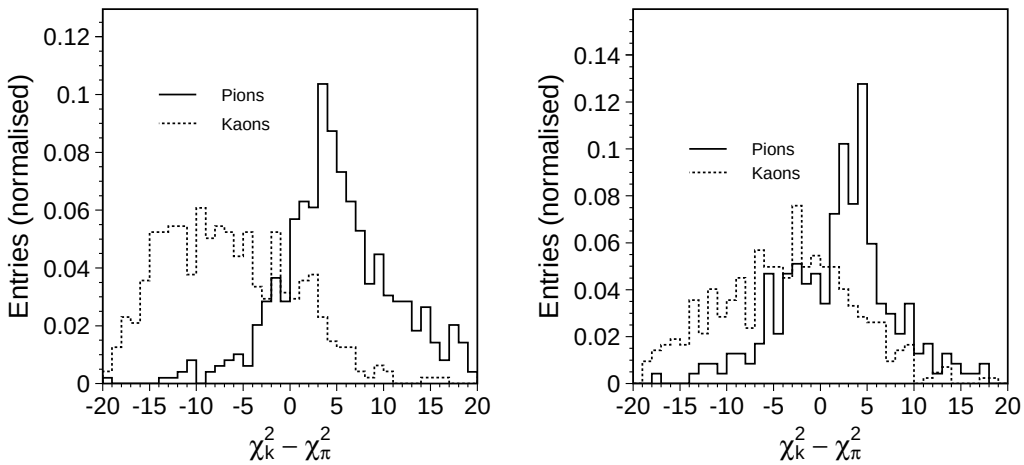

(a) 0, 1, 2 minimum bias interactions per bunch crossing

(b) 7, 8, 9 minimum bias interactions per bunch crossing

Figure A.6: $\chi^2_K - \chi^2_\pi$ The difference in the negative log-likelihoods for the Kaon and Pion hypotheses.

addition to the one that produces the B_s. (Poisson distributions were not used.) Runs with *imin* = 0, 1, 2, ..., 10 minimum bias events per signal events were done, and each was analyzed separately.

First we look at the difference in the negative log-likelihoods in the Kaon and Pion hypotheses ($\chi^2_K - \chi^2_\pi$) for the Kaons and Pions from the B_s decays. They are plotted in Fig. A.6(a) for 0, 1, 2 minimum bias events per bunch crossing and Fig. A.6(b) for 7, 8, 9 minimum bias interactions per bunch crossing. A cut of $\chi^2_K - \chi^2_\pi < 4.0$ was applied to identify Kaons.

It is clear that with a larger number of minimum bias events, the separation between Kaons and Pions becomes poorer. To keep the background minimal we require in this study a cut of $\chi^2_K - \chi^2_\pi < 4.0$ to identify Kaons independent of the number of interactions per bunch crossing.

Let us define ϵ_{imin} to be the efficiency within the event generation cuts, for a value of *imin*, the number of minimum bias events per signal event in the sample. It is measured for each value of *imin* minimum bias events per signal event in the sample. The numbers are normalized to the value at no (0) minimum bias events to get a relative efficiency.

By the above definition, the value of ϵ_{imin} at $imin = 0$ is 1.0. Thus, ϵ_{imin} is the scaled signal efficiency for a given value of *imin*, relative to the same quantity for $imin = 0$. This distribution is then fitted to an exponential function of the form $\exp(constant + slope \times x)$. This function then gives us the value of ϵ_{imin} for each value of *imin*. The distributions for ϵ_{imin} are shown in Fig. A.7(a) and Fig. A.7(b).

As mentioned, the efficiency ϵ_{imin} is obtained for each value of *imin* and is an efficiency

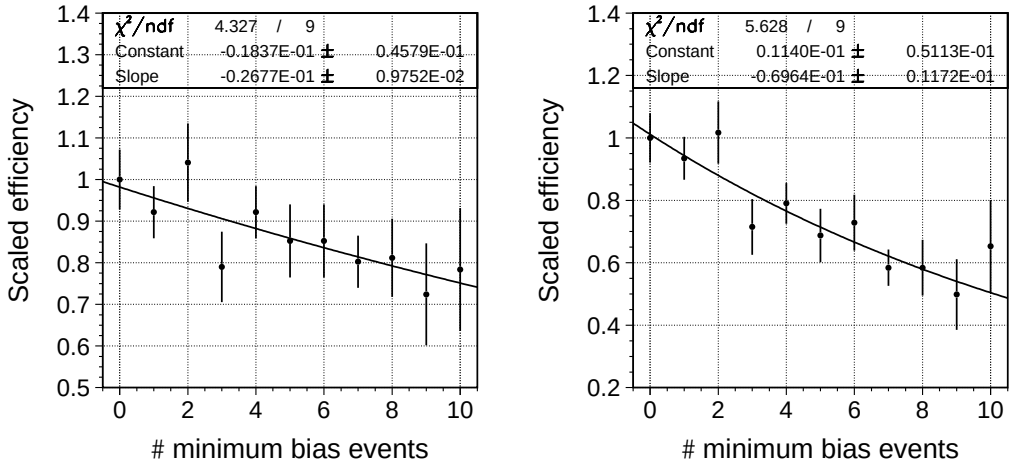

(a) At least one tagged Kaon from ϕ decays

(b) Both Kaons from ϕ decays are tagged

Figure A.7: The scaled efficiency (ϵ_{imin}) distributions, both fitted to exponentials as mentioned in the text.

within the event generation cuts mentioned above. This efficiency is convoluted with Poisson distributions of mean 2.0 and 6.0, to give the selection efficiencies at those luminosities. The important quantity here is the relative efficiency (ratio of the two convoluted numbers) which gives the change in performance as the luminosity is changed. We thus define

$$\epsilon_{\rm rel} = \frac{\sum \epsilon_{\rm imin} * {\rm Poisson}(6.0, {\rm imin})}{\sum \epsilon_{\rm imin} * {\rm Poisson}(2.0, {\rm imin})}$$

where Poisson is defined as

$$\text{Poisson}(\mu, \text{n}) = \frac{\mu^{\text{n}} \exp(-\mu)}{\text{n!}}$$

Here, ϵ_{rel} will provide us with the change in performance in the BTeV RICH detector, as measured in a change in the efficiency for our signal events. In the current analysis, ϵ_{rel} was measured for two cases: at least one kaon from ϕ decays being tagged and both the kaons being tagged.

ϵ_{rel} gives us the relative efficiency change in the BTeV RICH detector for our chosen signal. The result we obtained for events where at least one Kaon from ϕ decays is identified in the RICH is $\epsilon_{rel} = 0.90$ while $\epsilon_{rel} = 0.76$ for events where both the Kaons from ϕ decays are required to be identified.

We show in Table A.3 the relative particle identification efficiency for both the standard analysis case of identifying the fast K^- and one of the two kaons from the ϕ and also the more stringent case of identifying both kaons from the ϕ for different number of interactions per crossing.

<Int/crossing>	Bunch spacing (ns)	ϵ 2 Kaons	ϵ 3 Kaons
2	132	1.0	1.0
4	396	0.95	0.87
6	396	0.90	0.76

Table A.3: RICH particle identification efficiencies from different average number of interactions per crossing and either 2 (standard) or 3 (stringent) kaons identified, relative to the efficiency at 2 interactions/crossing.

<Int/crossing>	Bunch spacing (ns)	$\epsilon(K)$	$\epsilon(\pi)$	S/B
2	132	0.76	0.020	13
4	396	0.70	0.022	10
6	396	0.61	0.026	8

Table A.4: The efficiency for identifying the fast kaon in the decay $B_s \to D_s^{\pm} K^{\mp}$ and rejecting the fast pion from $B_s \to D_s^{\pm} \pi^{\mp}$ for different numbers of interactions per crossing. The signal to background after apply a B_s mass cut is also given.

For our standard analysis cuts we have relative efficiency of 95% at 396 ns relative to 132 ns at a luminosity of $2 \times 10^{32}\mathrm{cm}^{-2}\mathrm{s}^{-1}$. Even for the more stringent case of requiring that both kaons from the ϕ decay be identified (as well as the fast kaon), our efficiency loss is only 12%.

The second study was initiated to see how the backgrounds would influence our sensitivity. Here we generate both $B_s \to D_s^{\pm} K^{\mp}$ and $B_s \to D_s^{\pm} \pi^{\mp}$ events. The latter reaction is expected to be 15 times more prolific than the former and thus would be a major source of background. In this study the kaons from the ϕ were not identified. We have not optimized the identification cuts at each number of interactions, but merely apply the ones found at 2 interactions per crossing. We obtain the efficiencies for identifying kaons as kaons ($\epsilon(K)$) and mis-identifying pions as kaons ($\epsilon(\pi)$); these are shown in Table A.4. The signal to background ratio (S/B) is found by applying a B_s mass cut in addition.

The effects on our measurement of the CP violating angle γ can now be roughly estimated. The error on the CP asymmetry will be proportional to $\sqrt{\epsilon_K/(1+B/S)}$. We now normalize to 2 interactions per crossing and average over 2, 4 and 6 interactions. The final result is that error in the CP violating asymmetry is increased by 6%.

Both of these estimates show that the effects of running at 396 ns will not increase the error on the CP asymmetry in this channel by more than 6%; the decrease in the effective event rate is not more than 12%.

A.4.2 The liquid radiator system

The liquid radiator subsystem is used mainly to separate kaons from protons below a momentum of 9 GeV/c as neither radiate in the gas. The photo-detectors are 3″ diameter tubes, although it is possible to use 2″ diameter tubes, that would provide better segmentation at an increased cost.

We have investigated the effects of 6 interactions per crossing on the kaon efficiency versus proton fakes for samples of kaons used in flavor tagging fully reconstructed B_s events, useful for measurements of mixing and CP violation.

To select a sample of candidate tagging kaons, we first insist that they not be identified as pions in the gas subsystem. Then we need to separate the kaons from the protons. Figure A.8(a) shows the kaon efficiency versus proton rejection for the two samples of putative kaons, those selected with association to another detached vertex other than that of the B_s decay under consideration and those selected as coming from the primary interaction vertex and being close in phase space to the B_s.

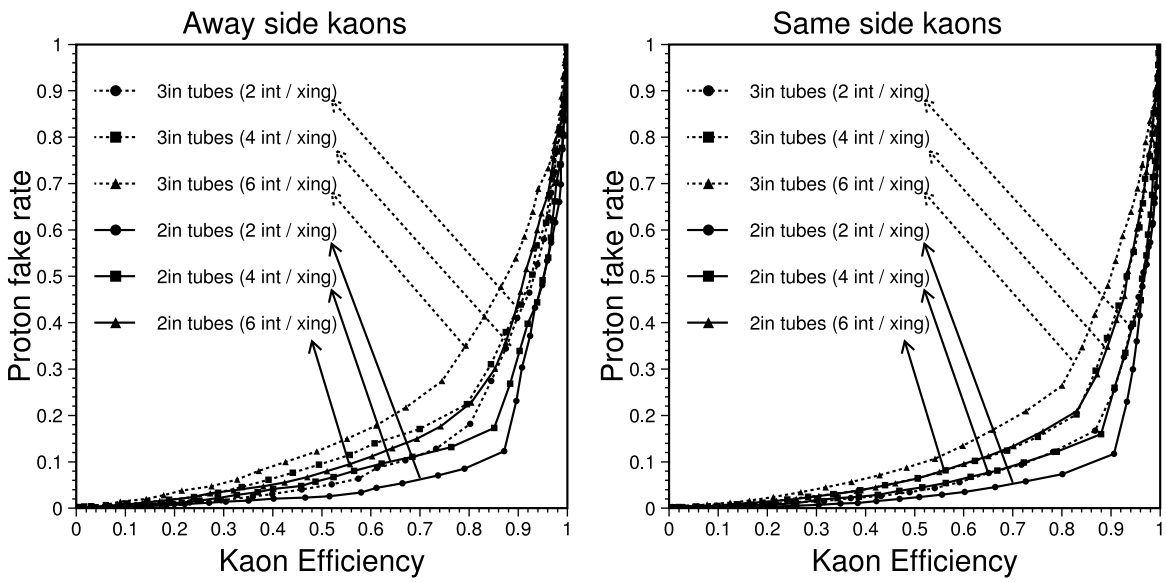

(a) Away side flavor tagging

(b) Same side flavor tagging

Figure A.8: Kaon efficiency versus proton rejection for a sample of kaons selected for use in flavor tagging and having momenta below 9 GeV/c.

We see that the larger number of interactions does in fact worsen the proton fake rates at fixed efficiency but the degradation is not very serious. We conclude that it is not worth the ∼1M$ to go the 2″ phototubes.

A.5 Effects on the Reconstruction of π^o's and η's by the Electromagnetic Calorimeter

A.5.1 Effects on $B \rightarrow \rho^+\pi^-$ due to changes in π^o's

Here we study the effects on the reconstructed B mass distribution for the channel $B^o \rightarrow \rho^+\pi^- \rightarrow \pi^+\pi^-\pi^o$. This mode probes the efficiency of the EM calorimeter.

We generate signal Monte Carlo events using GEANT containing a signal event with Poisson distributed minimum bias interactions with means either at 2, 4 or 6 interactions per crossing.

To select B^o-candidates we used the set of cuts described in the original BTeV Proposal-2000 (page 276) [5] . In particular, to select π^o-candidates we require that

- The energy of each $\gamma > 1$ GeV
- There must not be the projection of a charged track within 2 cm of the center-of-gravity of γ-candidate
- The energy of the π^0 (sum energy of the two γ's) must be > 5 GeV
- The transverse momentum p_t of the π^0 (vector sum of the transverse momenta of the two γ's) must be > 0.75 GeV

Shown in Fig. A.9 are the reconstructed three-pion mass distributions for 2, 4, and 6 interactions/crossing. The effects on the detection efficiency are small. However, there is an increase in multiple combinations from the same event. Specifically, For 2 interactions/crossing out of 225 entries there are 2 wrong $\pi^+\pi^-$ combination and 11 entries due to more than one photon-photon combination in the same event that passed our criteria for being a π^o from the B^0 decay.

For 4 interactions/crossing, out of 238 entries there is 1 wrong $\pi^+\pi^-$ combination and 18 entries due to multiple photon-photon combinations passing the cuts.

At 6 interactions/crossing, out of 287 resulting 3π-mass combinations there are 3 wrong $\pi^+\pi^-$ combinations, and there were 48 entries due to more than one photon-photon combination in the same event.

We can characterize these effects as the combinatorial background in signal events increasing from $\sim$5% to $\sim$20%. Since our model is to take data 1/3 of the time at each interaction rate, the effect is noticeable but not dominant.

We have also investigated the effects on the $\rho^+\pi^-$ background. In our previous study at 2 interactions per crossing we found 32 background events in the B mass interval from 4 to 7 GeV out of 9 million generated background events containing one B meson decay (not $\rho\pi$) along with a Possion distributed mean of 2 minimum bias events per crossing. In this study we merged this sample of B plus 2 minimum bias events with an additional sample of minimum bias events generated with a Poisson distributed average of 4 minimum bias interactions per crossing. Charged tracks in the merged events were projected onto the

calorimeter and photons were from both samples were added in. The analysis then proceeded as before. We find that the background increased from the original 32 events to 42 events. This represents a small but significant increase in the background level but demonstrates that the detector can produce good results at 6 interactions per crossing.

A.5.2 Effects on $B_s \to J/\psi\eta$ due to changes in η's

Here we study the effects on the reconstructed B mass distribution for the channel $B_s \to J/\psi\eta$. This channel is used to measure the CP violating angle χ and thus is of much importance. The electromagnetic calorimeter is crucial here as it is used to detect $\eta \to \gamma\gamma$.

Here we generate signal Monte Carlo events using GEANT containing a signal event with Poisson distributed minimum bias interactions with means either at 2, or 6 interactions per crossing.

Muon candidates are selected by being identified either in the muon detector for momenta above 10 GeV/c or in the RICH for muon momenta below 17 GeV/c. The opposite sign dimuon candidate invariant mass distributions are shown in Fig. A.10(a) and (b) at both 2 and 6 interactions per crossing.

We see that there is no visible effect on the reconstruction efficiency or the background level in the signal Monte Carlo sample from the increased number of interactions per crossing.

To select η's we use a slight different set of selection criteria than for selecting π^o's:

- We make the shower shape cuts - E1/E9 >0.65 and E9/E25 >0.95, where E_i are the highest i energy crystals in the shower
- The angle of each photon is required to be > 12 mrad.
- There must not be the projection of a charged track within 3 cm of the center-of-gravity of each γ-candidate
- The energy of each candidate photon is > 4 GeV
- The transverse momentum of each photon is required to be > 0.4 GeV/c

The invariant mass distributions of two candidate photons are shown in Fig. A.11(a) and (b) at both 2 and 6 interactions per crossing.

Here the effects of more interactions are quite noticeable. While the σ is about 6 MeV for 2 and 6 interactions per crossing, the resulting background level in the signal events is significantly higher for 6 interactions per crossing.

The effects on the B_s efficiency and resolution are shown in Fig. A.12(a) and (b). The efficiency is decreased by 8% and the resolution is not visibly affected. The background level is also somewhat increased. We conclude that averaging over 2, 4 and 6 interactions per crossing, the effects will be small, on the level of 4% decrease in our ability to extract the CP violation angle χ using this channel.

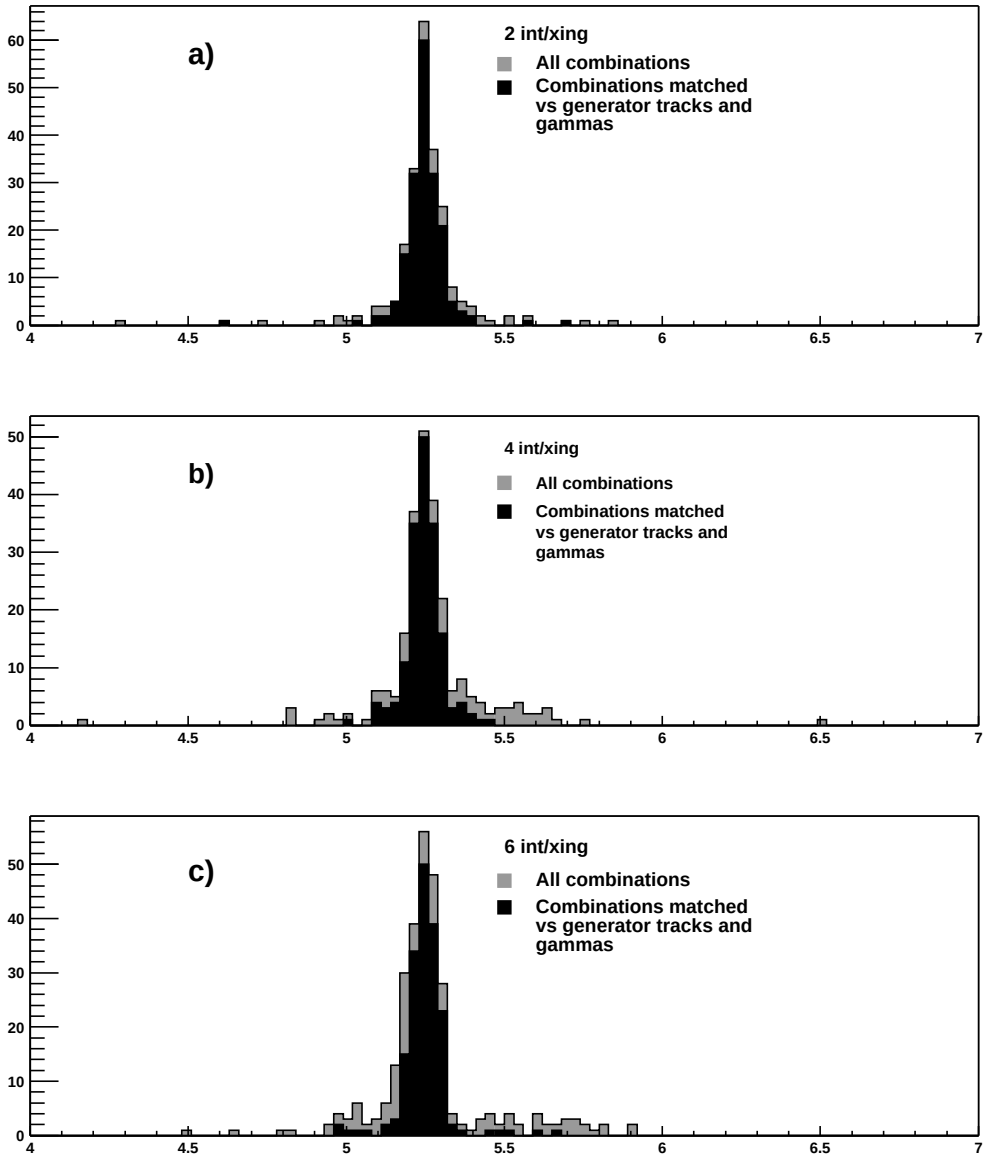

Figure A.9: Invariant mass $\pi^+\pi^-\pi^0$, in units of GeV. The darker histogram shows mass combinations matched to generator tracks and photons, while the lighter histogram includes all combinations.

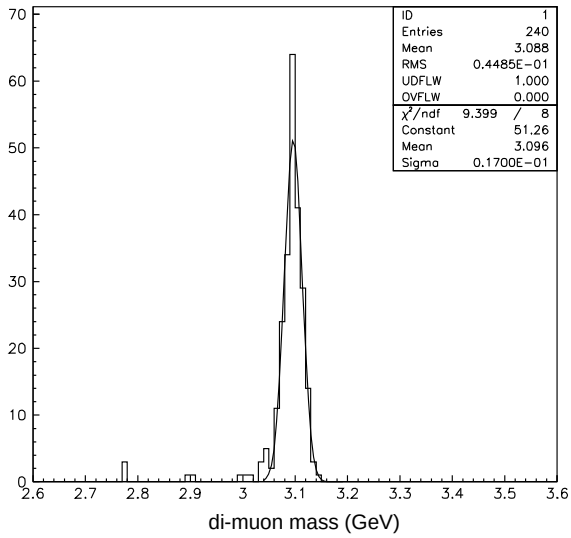

(a) Signal plus 2 minimum bias interactions per crossing

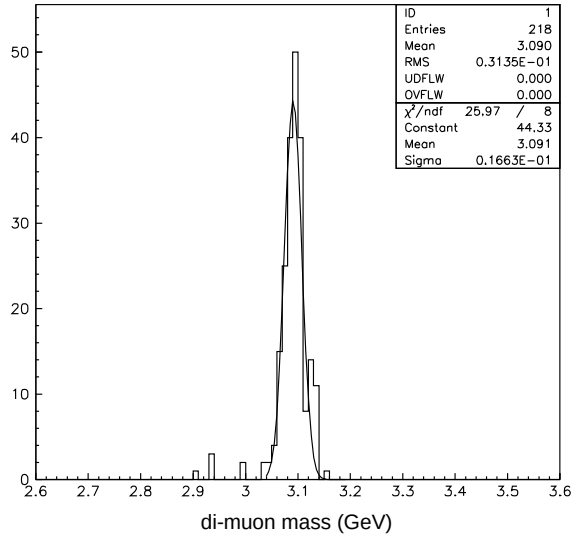

(b) Signal plus 6 minimum bias interactions per crossing

Figure A.10: Dimuon candidate invariant mass distributions for $B_s \to J/\psi\eta$ signal plus minimum bias interactions. The curves are fits to signal Gaussians whose means and widths are allowed to float.

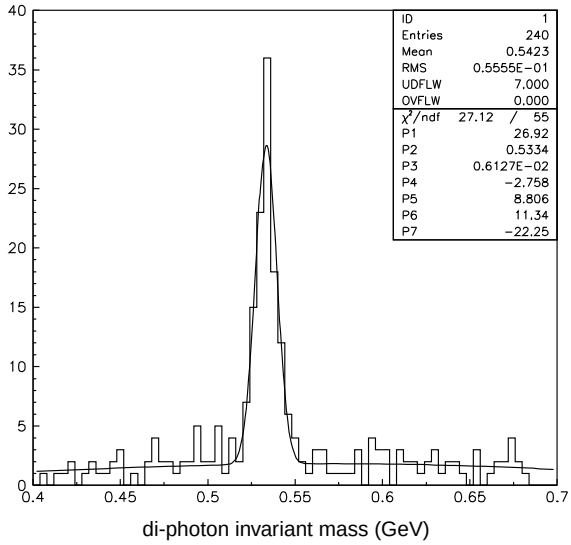

(a) Signal plus 2 minimum bias interactions per crossing

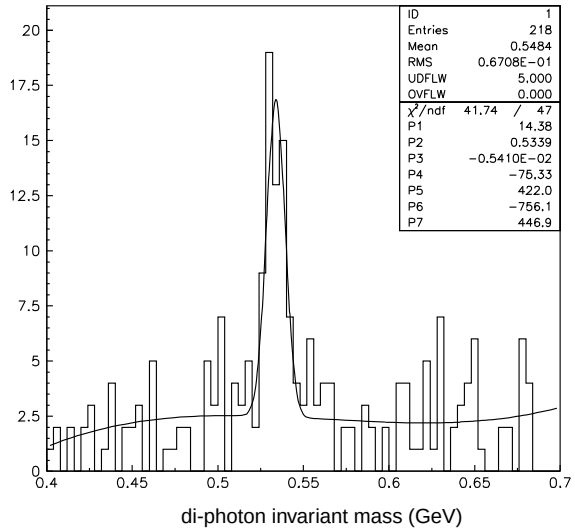

(b) Signal plus 6 minimum bias interactions per crossing

Figure A.11: Diphoton candidate invariant mass distributions for $B_s \to J/\psi\eta$ signal plus minimum bias interactions.

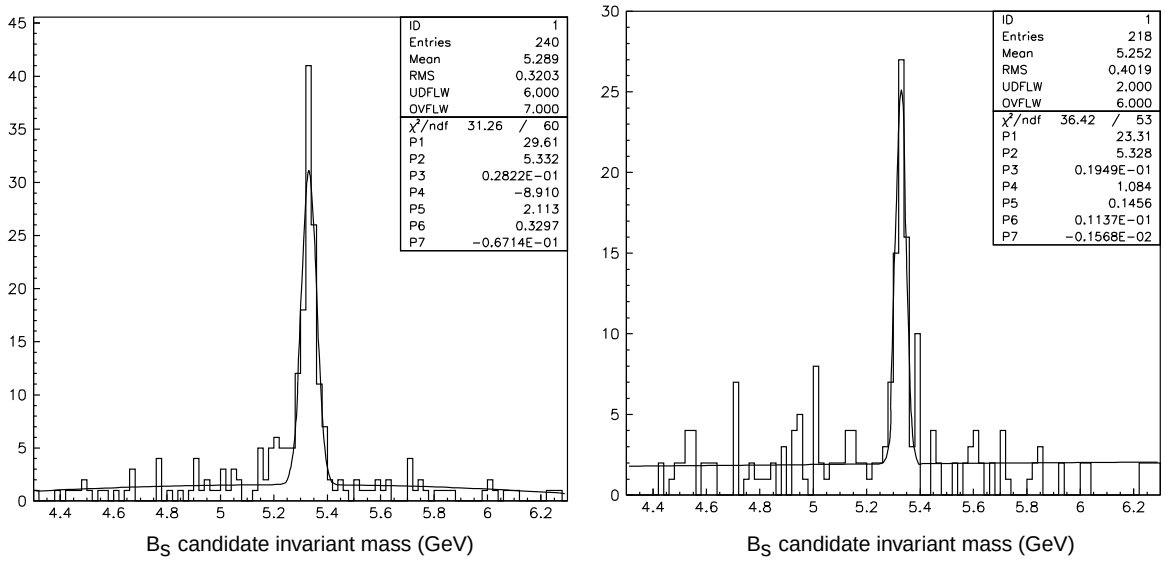

(a) Signal plus 2 minimum bias interactions per crossing

(b) Signal plus 6 minimum bias interactions per crossing

Figure A.12: $J/\psi\eta$ candidate invariant mass distributions for $B_s \to J/\psi\eta$ signal plus minimum bias interactions.

Bibliography

[1] http://warrior.lbl.gov:7778/pacfiles/papers/MONDAY/PM_ORAL/MOPA003/MOPA003.PDF

[2] The total cross-section is 77.6 mb. The elastic cross-section is 18.9 mb and the diffractive cross-section is 19.0 mb. Taking the total minus elastic and minus half the diffractive gives an inelastic cross-section of 49.2 mb. For 50 mb and $2 \times 10^{32}\mathrm{cm}^{-2}\mathrm{s}^{-1}$ we have 10^7 interactions per second. For 132 ns bunch spacing (7.6 MHz rate), we have 1.3 inelastic interactions per crossing.

[3] One caveat here is that it maybe possible to run with a "leveled" luminosity, that is one that doesn't change with time of the course of a store. This is achieved by slightly defocusing the beam at the start of the collisions, to produce a lower initial luminosity, and then tightening the focus as the intensity of the beams declines to keep it roughly constant. If that happened it would likely be an a more constant rate but still having an average corresponding to 3-4 interactions per crossing.

[4] The BTeV Proposal Update may be found at http://www-btev.fnal.gov/cgi-bin/public/DocDB/ShowDocument?docid=316

[5] The BTeV Proposal may be found at http://www-btev.fnal.gov/DocDB/0000/000066/002/index.html